Thin Solid Films 600 (2016) 13–18

Contents lists available at ScienceDirect

Thin Solid Films

journal homepage: www.elsevier.com/locate/tsf

Effect of doping behaviors of Ag and S on the formation of p-type Ag–S co-doped ZnO film by a modified hydrothermal method

Shiwang Long [a,b], Yongfeng Li [a,b,*], Bin Yao [a,b,*], Zhanhui Ding [a], Ying Xu [a,b], Gang Yang [b], Rui Deng [c], Zhenyu Xiao [a,b], Dongxu Zhao [d], Zhenzhong Zhang [d], Ligong Zhang [d], Haifeng Zhao [d]

[a] State Key Lab of Superhard Materials, Department of Physics, Jilin University, Changchun 130012, China
[b] Key Lab of Physics and Technology for Advanced Batteries, Ministry of Education, Department of Physics, Jilin University, Changchun 130012, China
[c] School of Materials Science and Engineering, Changchun University of Science and Technology, Changchun 130022, China
[d] State Key Lab of Excited State Processes, Changchun Institute of Optics, Fine Mechanics and Physics, Chinese Academy of Sciences, Changchun 130033, China

ARTICLE INFO

Article history:
Received 22 March 2015
Received in revised form 16 November 2015
Accepted 26 December 2015
Available online 5 January 2016

Keywords:
ZnO
p-Type doping
Thin film
Hydrothermal method

ABSTRACT

Reproducible p-type Ag–S co-doped ZnO (ASZO) films were grown on glass substrate by a modified hydrothermal method, where reaction solution is separated from alkali solution and O_2 is removed from autoclave to avoid deoxidation of Ag^+ and oxidation of S^{2-} in the solution. It is found that the Ag substitutes for the Zn in monovalent state (Ag_{Zn}^{+}) and the S for the O in bivalent state (S_O^{2-}) in the ASZO. Both Ag_{Zn}^{+} and S_O^{2-} have two doping states, each Ag_{Zn}^{+} is surrounded by $4O^{2-}$ to form Ag_{Zn}^{+} acceptor and each S_O^{2-} is surrounded by 4_{Zn}^{2+}, while Ag_{Zn}^{+} bounds with nS_O^{2-} to form Ag_{Zn}^{+}–nS_O^{2-} ($n \le 4$) complex acceptor. It is demonstrated that Ag doping can suppress the formation of interstitial Zn and O vacancies in the ASZO and S doping can enhance solubility of Ag in the ASZO. Hall measurement indicates that the p-type ASZO film has a hole density as high as 10^{18} cm^{-3}, which is much higher than that of ASZO prepared by magnetron sputtering. The mechanism of the formation of the p-type ASZO with high hole density is suggested in the present paper.

1. Introduction

ZnO is a wide band gap semiconductor with a band gap of 3.27 eV and is considered as candidate for the preparation of short wavelength light emission diodes (LEDs), laser diodes (LDs), and photodetectors [1–14]. However, strong self-compensating effect, low acceptor doping content and deep acceptor level make it quite difficult to fabricate stable p-type ZnO reproducibly, and become the key scientific issues in the field of ZnO [15–17]. In the past 15 years, many research works are carried out on fabrication of p-type ZnO through replacing lattice Zn atoms by Group IA (Li, Na) elements [18], or lattice O atoms by Group V (N, P and As) elements [19–20], or co-doping [21–22], but there still exist the problems of poor reproducibility, conductivity and stability in the p-type doped ZnO. Besides the self-compensation effect of native donors, low doping content and deep acceptor level, there is a self-compensation effect induced by the acceptor dopant, for example, the compensation of interstitial Li donor for acceptor produced by substitution of Li for Zn in Li-doped ZnO, which results in that the Li-doped ZnO is usually n-type conducting or semi-insulating. So, it is also an important problem to avoid the self-compensation induced by dopant through selection of suitable acceptor dopant.

Yan et al. indicated that Ag may be a good candidate for fabricating p-type ZnO due to the fact that the formation energy of substitution of Ag^{1+} for Zn (Ag_{Zn}^{+}) is smaller than that of interstitial Ag (Ag_i), based on first-principles calculation [23], which can avoid self-compensation induced by acceptor dopant (compensation of Ag_i donor for Ag_{Zn}^{+} acceptor). However, the ionization energy of the Ag_{Zn}^{+} acceptor (0.444 eV) is too high for achieving p-type conductivity. Persson et al. indicated that the strong VB offset bowing of $ZnO_{1-x}S_x$ alloy can be utilized to decrease the ionization energy of acceptor doped in the ZnO-like alloys [24], which was used by some research groups to prepare p-type ZnO through Ag–S co-doping using the RF magnetron sputtering technique [25–26]. Although the Ag–S co-doped ZnO prepared by magnetron sputtering shows a better p-type conductivity and stability, its hole density of 10^{15}–10^{16} cm^{-3} is still low for application in an optoelectronic device. The low hole density may be due to the existence of many intrinsic donor defects and poor crystal quality of the Ag–S co-doped ZnO film, because the film produced by magnetron sputtering is grown in a non-equilibrium thermodynamic process.

It is known that ZnO films are grown under non-equilibrium thermodynamic state in many preparation technologies, for example, magnetron sputtering and spin-coating, and that only growth temperature can be used to tune defects and crystal quality of the films. Therefore, they usually have a large amount of intrinsic defects, poor crystal quality and poor optical and electrical properties. Hydrothermal method is a convenient, cheap and environmentally friendly method and is used to prepare

* Corresponding authors at: State Key Lab of Superhard Materials, Department of Physics, Jilin University, Changchun 130012, China.
E-mail addresses: liyongfeng@jlu.edu.cn (Y. Li), binyao@jlu.edu.cn (B. Yao).

http://dx.doi.org/10.1016/j.tsf.2015.12.070
0040-6090/

ZnO film successively. Since growth of film is in quasi-equilibrium thermodynamic state in the hydrothermal process and species and amount of the intrinsic defects are related to preparation techniques, it can be expected that the ZnO film produced by the hydrothermal method would have good crystal quality, less intrinsic defects, different distribution of intrinsic defects, and good electrical properties, compared to the ZnO films produced by magnetron sputtering, etc.

Based on the alkali source used in the synthesis of ZnO, the hydrothermal systems reported previously can be separated into three kinds: organic, inorganic and no alkali source systems. However, the former two systems usually are strongly alkaline or contain oxidizer and deoxidizer, which may make Ag^+ be deoxidized (especially when the solution is heated), or S^{2-} to be oxidized, resulting in that the Ag and S incorporate into ZnO difficultly in ionic states. ZnO cannot be synthesized continuously in the system without alkali source and it is hard to control the morphology of ZnO film. Therefore, the hydrothermal systems reported previously for the preparation of ZnO are not suitable for fabricating the Ag–S co-doped ZnO thin film. It is necessary to modify the hydrothermal systems. However, there are few papers on the preparation of Ag- or S-doped ZnO by the hydrothermal method [27–28].

In the present work, p-type Ag–S co-doped ZnO with high hole density was prepared by using the modified hydrothermal method, the doping behaviors of Ag and S and its effects on intrinsic defects and solubility of ZnO were characterized, and formation mechanism of the p-type Ag–S co-doped ZnO was suggested.

2. Experimental methods

All films used in this work, including un-doped ZnO (ZnO), Ag-doped ZnO (AZO), S-doped ZnO (SZO) and Ag–S co-doped ZnO (ASZO), were grown on glass substrate coated with a layer of ZnO seed by using the modified hydrothermal system described below, the ZnO seed layer was fabricated by the spin-coating technique [14].

Sketch of the inside structure of the modified hydrothermal system is shown in Fig. 1. Reaction solution consists of a small amount of pyridine (C_5H_5N, 99.5%) and zinc, silver, sulfur sources or their mixtures, as listed in Table 1, as well as conditioning agent. The reaction solution is filled in the liner of autoclave. Alkali solution is composed of butylamine ($CH_3(CH_2)_3NH_2$, 99.5%) and C_5H_5N. In order to avoid deoxidization of Ag^+, the alkali solution is separated with the reaction solution by filling it in a volumetric flask, as shown in Fig. 1. When the autoclave is heated, the surface of the reaction solution rises up, the reaction solution vaporizes and the Brownian movement in reaction solution becomes stronger, resulting in an increase in the pressure of the autoclave. As the autoclave is heated to some fixed temperature (usually above 100 °C), a zone that has strong convection comes into being near the interface of gas and reaction solution, which will absorb the vaporized alkali into the zone to react with the reaction solution, forming ZnO or Ag-doped or Ag–S co-doped ZnO. This method also can be used to fabricate other kinds of metal oxides or metal hydroxides.

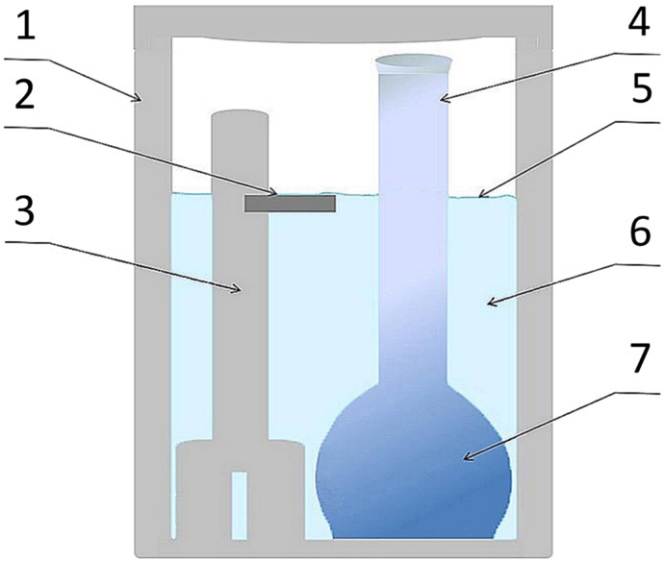

Fig. 1. Sketch of the inside structure of the autoclave. 1. PTFE liner; 2. substrate; 3. PTFE stand; 4. volumetric flask; 5. the surface of reaction solution; 6. reaction solution; 7. alkali solution.

Table 1 shows starting materials and their concentrations for the preparation of various samples. For un-doped ZnO films, the reaction solution is prepared by dissolving zinc salt(s) (zinc nitrate hexahydrate, $Zn(NO_3)_2\cdot 6H_2O$, 99.0%) or mixture of $Zn(NO_3)_2\cdot 6H_2O$ and zinc acetate dihydrate ($Zn(Ac)_2\cdot 2H_2O$, 99.0%) and ammonium nitrate (NH_4NO_3, 99.5%) with deionized water in an ultrasonic bath and then adding a small amount of C_5H_5N. Here, NH_4NO_3 served as a conditioning agent. The glass substrate with a layer of ZnO seed on one side was placed horizontally onto the surface of the reaction solution using a polytetrafluoroethylene (PTFE) stand, and the side with ZnO seed faces down the solution. The alkali solution is filled in the volumetric flask. The autoclave with the reaction solution, glass substrate and alkali solution is closed and then heated at 190 °C for 1 h in a thermostatic drier. Finally, the glass substrate with undoped ZnO thin film is rinsed in deionized water and dried at 120 °C for 10 min. For Ag-doped ZnO films, silver nitrate ($AgNO_3$, 99.8%) was added to the reaction solution mentioned above for un-doped ZnO to serve as a silver source; for S-doped ZnO films, tetramethylthiourea (TMTU, 98.0%) was added to the reaction solution to serve as a sulfur source, and high purity N_2 gas (99.99%) was filled into the liner in order to avoid oxidation of S^{2-}; for Ag–S co-doped ZnO, TMTU and silver chloride (AgCl, 99.5%) were added to the reaction solution to serve as a sulfur source and silver source, respectively, and high purity N_2 gas was filled into the liner in order to avoid oxidation of S^{2-}. TMTU is a strong ligand of Ag^+ and hydrolyzes at the temperature above 160 °C to release hydrogen sulfide (H_2S). And H_2S ionizes and reacts with Ag^+ to form coordination complex $[Ag(HS)_2]^-$, which was designed to introduce Ag_{Zn}^{+}–nS_O^{2-} ($n \le 4$) into ZnO. The doping content was controlled by changing the mole ratios of S source to Zn source and Ag source to Zn source in the reaction solution. In the present work, the formation of the Ag–S co-doped ZnO can be expressed by following chemical equations:

$$AgNO_3 \rightarrow Ag^+ + NO_3^- \quad (1)$$

$$AgCl + 3TMTU \rightarrow [Ag(TMTU)_3]^+ + Cl^- \quad (2)$$

$$[Ag(TMTU)_3]^+ + 2H_2O \xrightarrow{\Delta} [Ag(HS)_2]^- + 2TMU + TMTU + 2H^+ \quad (3)$$

$$TMTU + H_2O \xrightarrow{\Delta} TMU + H_2S \quad (4)$$

$$H_2S \rightarrow HS^- + H^+ \quad (5)$$

$$NH_4^+ + C_5H_5N \rightleftarrows NH_3 + C_5H_6N^+ \quad (6)$$

$$NH_4^+ + CH_3(CH_2)_3NH_2 \rightarrow NH_3 + CH_3(CH_2)_3NH_3^+ \quad (7)$$

$$NH_3 + H_2O \rightleftarrows NH_4^+ + OH^- \quad (8)$$

$$CH_3COO^- + H_2O \rightleftarrows CH_3COOH + OH^- \quad (9)$$

$$Zn^{2+} + 2OH^- \rightarrow Zn(OH)_2 \quad (10)$$

$$Zn(OH)_2 \xrightarrow{\Delta} ZnO + H_2O \quad (11)$$

Table 1
Starting materials and their concentrations for the preparation of various samples.

Sample	$Zn(NO_3)_2 \cdot 6H_2O$ (mM)	$Zn(Ac)_2 \cdot 2H_2O$ (mM)	$AgNO_3$ (mM)	TMTU (mM)	AgCl (mM)
(ZnO-I) un-doped ZnO-I	100	–	–	–	–
(ZnO-II) un-doped ZnO-II	25	75	–	–	–
(SZO-I) S-doped ZnO-I	25	75	–	50	–
(SZO-II) S-doped ZnO	25	75	–	100	–
(SZO-III) S-doped ZnO	25	75	–	200	–
(AZO-I) Ag-doped ZnO-I	100	-	0.5	–	–
(AZO-II) Ag-doped ZnO-II	100	-	1	–	–
(ASZO-I) Ag–S co-doped ZnO-I	25	75	–	100	2
(ASZO-II) Ag–S co-doped ZnO-II	25	75	–	100	5
(ASZO-III) Ag–S co-doped ZnO-III	25	75	–	100	10
(ASZO-IV) Ag–S co-doped ZnO-IV	25	75	–	100	20

$$ZnO + \left[Ag(HS)_2\right]^- \rightarrow ZnO : (Ag, S) + 2OH^- \quad (12)$$

where TMU is tetramethylurea.

The composition of the films was investigated by Energy Dispersive Spectrometer (EDS, Hitachi MPF-4). 15 kV voltage was applied as EDS measurement was performed. To characterize the structures of the un-doped and doped ZnO thin films, the standard θ–2θ scanning was performed by X-ray diffraction (XRD) with Cu Kα radiation source (λ = 1.5406 Å). Electrical properties were measured by a Hall effect measurement system (LakeShore7707) at room temperature in the van der Pauw configuration. Photoluminescence (PL) was measured at room temperature by using the UV Labran Infinity Spectrophotometer with He–Cd laser line of 325 nm as an excitation source. To detect the composition and chemical states of elements, the film samples were tested using the X-ray photoelectron spectroscopy (XPS) by ESCALAB 250 XPS instrument with an Al *Kα* ($h\nu = 1486.6$ eV) X-ray radiation source which had been carefully calibrated by the C 1s peak (284.6 eV).

3. Results and discussion

In order to understand electrical properties of the ASZO and related mechanism, Hall measurement was performed for the ZnO, SZO, AZO and ASZO films, and the results are listed in Table 2. It can be seen from Table 2 that both the ZnO and SZO show n-type conduction, but the electron density of SZO is about one order of magnitude smaller than that of ZnO. However, for AZO, although it still shows n-type conduction when nominal mole ratio of Ag source to Zn source is 0.5% in the reaction solution, its electron density dropped dramatically from 10^{18} to 10^{15} cm^{-3}. Moreover, when the nominal ratio increases to 1%, the AZO converts from n-type to p-type, but the p-type conductivity is not stable and poor, that is, it spontaneously turns from p-type to n-type after several days or weeks. For the ASZO, when the nominal mole ratio of S source to Zn source increases to 100:100 and nominal mole ratio of Ag source to Zn source increases to 5–20%, it shows p-type conductivity with a hole density of 10^{17}–10^{18} cm^{-3}, and the hole density increases and resistivity decreases with increasing the nominal mole ratio of the Ag source to Zn source. Interestingly, the ASZO film still shows a p-type conduction after half one year. Therefore, the p-ASZO film shows a better p-type conduction than the AZO film. It should be noted that the low Hall mobility is ascribed to the scattering of impurities or defects on carriers.

Table 2
Hall effect measurement results of undoped, Ag-doped, S-doped and Ag–S co-doped ZnO films.

Sample	Carrier type	Resistivity (Ω cm)	Carrier density (cm^{-3})	Mobility ($cm^2 V^{-1} s^{-1}$)
ZnO-I	n	2.3×10^1	2.7×10^{18}	3.2×10^{-1}
ZnO-II	n	2.5×10^1	4.3×10^{18}	5.7×10^{-2}
SZO-I	n	8.5	3.6×10^{18}	2.5×10^{-1}
SZO-II	n	5.5×10^1	3.3×10^{17}	2.7×10^{-1}
SZO-III	n	1.6×10^1	8.0×10^{17}	5×10^{-1}
AZO-I	n	9×10^3	3×10^{15}	6.5×10^{-1}
AZO-II	p	4.5×10^3	7.1×10^{15}	2.6×10^{-1}
ASZO-I	n	3.1×10^1	7.5×10^{17}	3.5×10^{-1}
ASZO-II	p	6×10^1	6.3×10^{17}	2.1×10^{-1}
ASZO-III	p	3.9	1.7×10^{18}	1.3
ASZO-IV	p	2.2	5.3×10^{18}	5.7×10^{-1}

To further verify the reliability of p-type conductivity of the ASZO films, a ZnO homojunction was fabricated by using n-type ZnO and p-type ASZO, as shown in the top-left inset in Fig. 2. The current–voltage (I–V) curve of the homojunction was measured at room temperature, as shown in Fig. 2. It reveals a typical rectification characteristic of diode. Prior to the I–V measurement of the homojunction, I–V curve of electrode contact on p-type ASZO was measured, as shown in the bottom-right inset in Fig. 2, indicating that the contact is an ohm contact. Therefore, the rectification characteristic comes from the homojunction, confirming that the p-type conductivity of the ASZO is reliable.

It is noted that the highest hole density of the p-type ASZO (10^{18} cm^{-3}) is two orders of magnitude higher than that of Ag–S codoped ZnO prepared by magnetron sputtering (ASZO-MS) (10^{16} cm^{-3}), moreover, the reproducibility of the p-type ASZO film reaches about 80%, which is also much higher than that of p-type ASZO-MS. Therefore, it is deduced that the modified hydrothermal method may be a good technique of the preparation of stable p-type ZnO.

It is well known that electrical properties of a semiconductor are related to its intrinsic defects and extrinsic impurities. In order to understand the mechanism of the formation of the p-type ASZO with high hole density, stability and reproducibility, characterizations for the structure of the undoped and doped ZnO films, doping behaviors of Ag and S in the ZnO and effects of the behaviors on the intrinsic defects are performed. Table 3 shows elements and their concentration of some typical samples measured by EDS, indicating that there are Ag, S and Ag and S elements in the nominal AZO, SZO and ASZO films, respectively. It is worth noting from Table 3 that Ag concentration in the ASZO is larger than that in the AZO and the Ag concentration increases with increasing S concentration, which imply that S doping can improve Ag concentration in ZnO film.

However, although EDS measurement can demonstrate that the doped ZnO films have Ag or/and S, it cannot demonstrate whether Ag or/and S incorporate into ZnO. In order to resolve this problem, XRD measurement is used to detect the doping behavior of Ag and S in the ZnO films. Fig. 3 shows the XRD patterns of the un-doped and doped ZnO films. The XRD pattern of the ZnO film shows a strong (002) diffraction peak of ZnO with wurtzite structure, while other diffraction peaks of ZnO are very weak, as shown in Fig. 3(a), indicating that the ZnO film is the preferred orientation in (002) direction. Fig. 3(b)–(e) shows the XRD patterns of SZO, AZO and two ASZO films with different Ag and S contents (ASZO-II and ASZO-III), respectively, which show that a strong diffraction peak is observed near diffraction angles of (002) peak of ZnO. Comparing with (002) peak of the ZnO films, the diffraction angles of

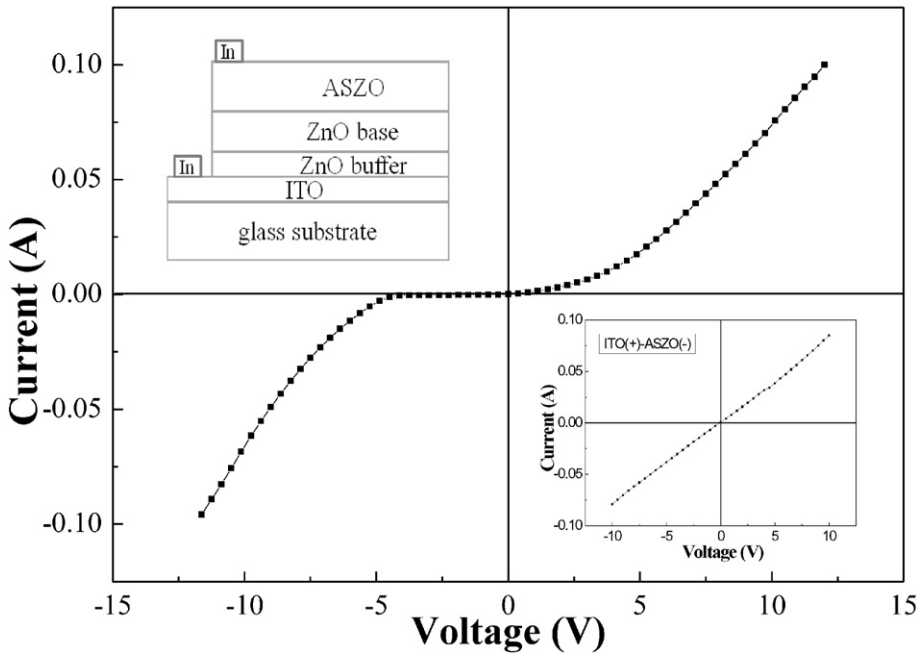

Fig. 2. The I–V curve of the ZnO p–n homojunction. The top-left and bottom-right insets show the diagram of the structure of the p–n homojunction and the I–V curve of electrode contact on p-type ASZO, respectively.

the peak of the SZO, AZO, ASZO-II and ASZO-III shift all to lower diffraction angle direction and decrease with increasing Ag or/and S contents, that implies that Ag or/and S incorporate into ZnO to form solid solution of ZnO and all the doped ZnO films consist of the solid solution of ZnO with (002) preferential orientation. It should be noted that all (002) diffraction peaks show significant asymmetry. The shoulder at the high angle side of the main peak leads to the asymmetry, which is derived from the $K_{\alpha 2}$ X-ray source. It is known that the Ag occupies the Zn site (Ag_{Zn}) and the S occupies the O site (S_O) in the Ag or S-doped ZnO [23]. For S doping, since S has only one chemical state of S^{2-} and ionic radius of S^{2-} (0.184 nm) is larger than that of O^{2-} (0.140 nm), substitution of S^{2-} for O^{2-} will result in an increase in lattice constant, that is, the shift of (002) diffraction peak towards lower angle direction, as shown in Fig. 3(b). So, the S doping state can be determined by the XRD to be occupying the O site in the chemical state of S^{2-} (denoted as S_O^{2-}). However, since Ag has two chemical states of Ag^{1+} and Ag^{2+} and the ionic radii of both Ag^{+} (0.115 nm) and Ag^{2+} (0.094 nm) are larger than that of Zn^{2+} (0.074 nm), the substitution of both for Zn leads to an increase in lattice constant c or shift of the (002) diffraction peak towards lower angle direction, as shown in Fig. 3(c). So, the chemical state of the Ag_{Zn} cannot be determined only by the XRD results.

In order to characterize the chemical state of the Ag and S-doped in ZnO, XPS was employed to detect the composition of the ASZO and chemical states of Ag and S in the ASZO. Fig. 4(a) shows that the calibrated C 1s peak is located at 284.6 eV. Fig. 4(b) and (c) shows the Zn 2p and O 1s peaks. Fig. 4(d) and (e) shows the XPS spectra of the Ag 3d and S 2p of the ASZO, respectively. The asymmetric Ag $3d_{5/2}$ peak can be disassembled into two sub-peaks centered at 367.5 and 368.0 eV, respectively, as shown in Fig. 4(d). The 367.5 eV is closed to the value of Ag $3d_{5/2}$ in Ag_2O, while 368.0 eV is closed to the value of Ag $3d_{5/3}$ in Ag_2S [29–30], indicating that the Ag_{Zn} is not in the chemical state of Ag^{2+} but Ag^{1+}. The spectrum of S 2p can be fitted by four sub-peaks, centered at 160.3, 161.4, 161.8 and 162.9 eV, respectively, as shown in Fig. 4(e). The 160.3 and 161.4 eV are closed to values of S $2p_{3/2}$ and S $2p_{1/2}$ in Ag_2S, respectively, while 161.8 and 162.9 eV are closed to values of S $2p_{3/2}$ and S $2p_{1/2}$ in ZnS, respectively. The XPS results indicate that Ag and S incorporate into ZnO in the chemical state of Ag_{Zn}^{+} and S_O^{2-} in the ASZO, respectively, and both have two doping states. One is the Ag_{Zn}^{+} with a binding energy of 367.5 eV surrounded by $4O^{2-}$ to form an acceptor (denoted by Ag_{Zn}^{+}) and the S_O^{2-} with S $2p_{3/2}$ of 161.8 eV surrounded by $4Zn^{2-}$ (denoted as S_O^{2-}), and the other one is Ag_{Zn}^{1+}.with a binding energy of 368.0 eV surrounded by nS_O^{2-} with S $2p_{3/2}$ of 160.3 eV (n is integral number less than 4) to form complex defect, which is denoted by Ag_{Zn}^{+}–nS_O^{2-}.

According to the discussion mentioned above, it is deduced that Ag has one doping state of Ag_{Zn}^{+} in AZO and two doping states of Ag_{Zn}^{+} and Ag_{Zn}^{+}–nS_O^{2-} in the ASZO. Both Ag_{Zn}^{+} and Ag_{Zn}^{+}–nS_O^{2-} complex act as acceptors [26,31], they may compensate donor defects to decrease background electron concentration or provide hole to increase hole density in the AZO and ASZO. The higher the amount of Ag-doped, the lower the background electron concentration or the higher the hole density of p-type ZnO. However, it is found that the electron concentration of n-type Ag-doped ZnO prepared by magnetron sputtering (denoted as ASZ-MS) (10^{17} cm^{-3}) is higher than that of the n-type AZO prepared in the present work (10^{15} cm^{-3}) and that the hole density of the p-type ASZO (10^{18} cm^{-3}) is much higher than that of the p-type ASZO-MS (10^{16} cm^{-3}) [31], even though the doping content of Ag in the AZO-MS and ASZO-MS are larger than that in the AZO and ASZO. These imply that the electrical properties of the Ag-doped and Ag–S co-doped ZnO are also affected by other factors except for the doping content and chemical state of Ag in ZnO.

It is known that intrinsic defects are important factors affecting electrical properties of semiconductors except for extrinsic impurities and that the formation of intrinsic defects is not only related to the thermodynamic formation but also to the preparation technique. In order to understand the effect of intrinsic defects on electrical properties of the AZO and ASZO, PL measurement was carried out at room temperature. Fig. 5 shows the room temperature PL spectra of the ZnO, AZO, SZO

Table 3
Elements and their concentrations for the various samples.

Sample	Zn (%)	O (%)	S (%)	Ag (%)
ZnO-II	51.2	48.8		
SZO-II	47.2	52.5	0.3	
SZO-III	48.4	51.0	0.6	
AZO-I	48.4	51.4		0.2
AZO-II	49.4	50.4		0.2
ASZO-II	48.1	50.7	0.4	0.8
ASZO-III	47.7	50.4	0.7	1.2

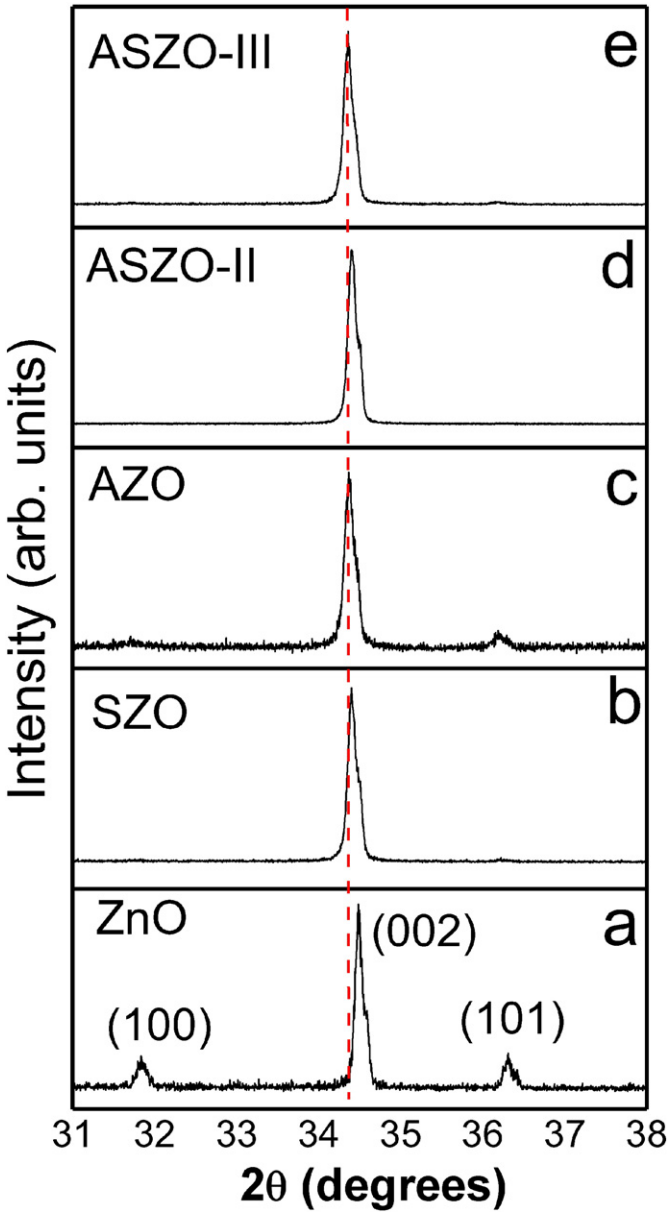

Fig. 3. XRD patterns of (a) ZnO, (b) SZO, (c) AZO, (d) ASZO-II, and (e) ASZO-III.

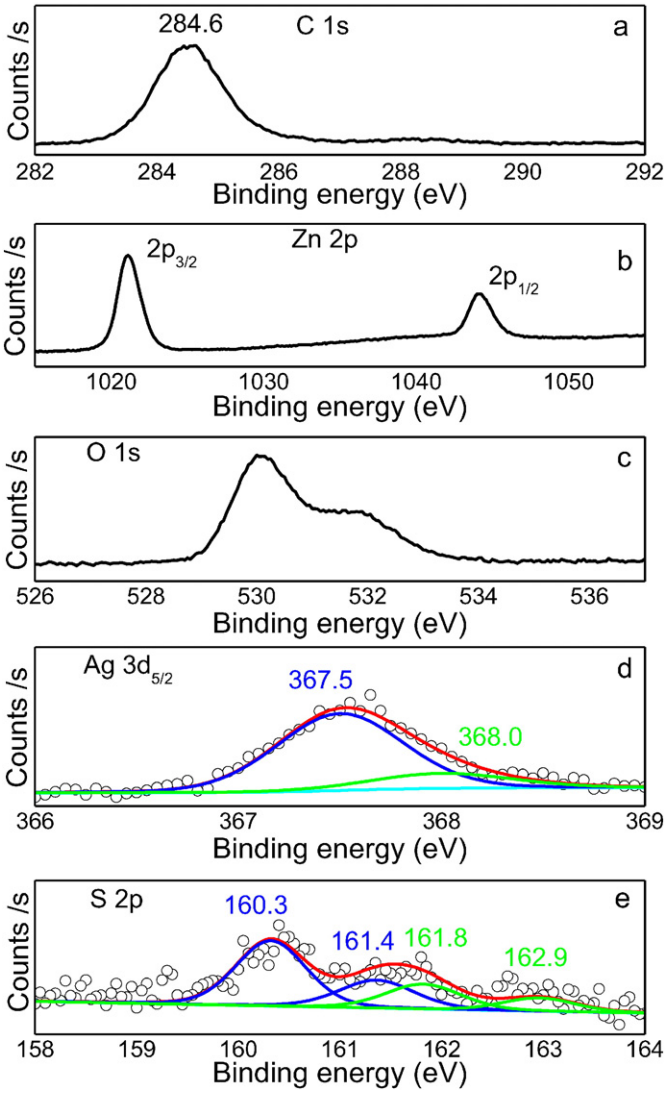

Fig. 4. C 1s (a), Zn 2p (b), O 1s (c), Ag $3d_{5/3}$ (d) and S 2p (e) XPS spectra of the ASZO.

and ASZO films. Two PL bands are observed at 3.27 and 2.06 eV in the PL spectrum of the ZnO, respectively, the former is due to near-band-edge emission of ZnO and the latter to electron transition from Zn_i to interstitial O (O_i) [32–33]. Since the ZnO is Zn-rich (as shown in Table 3) and shows n-type conduction with electron concentration of 10^{18} cm^{-3}, the Zn_i donor is a dominant intrinsic defect in the ZnO. When S dopes in ZnO, the 2.06 eV band disappears but a strong PL band appears at 2.45 eV, as shown in PL spectrum denoted by SZO, moreover, the composition of ZnO also changes from Zn-rich to Zn-poor, as shown in Table 3, which implies that the disappearance of the 2.06 eV band is attributed to a decrease in the Zn_i. The 2.45 eV band is attributed to electron transition from conduction band to O vacancy (V_O) level [32–33], so the appearance of the 2.45 eV band indicates the formation of many V_O defects. The above results indicate that S doping can suppress the formation of Zn_i but improve the formation of V_O, which makes the dominant intrinsic defect change from Zn_i to V_O. Since both Zn_i and V_O are donors and the ionization energy of Zn_i is smaller than that of V_O, the SZO should show n-type conduction with an electron density smaller than that of the ZnO, in agreement with Hall measurement result shown in Table 2. However, when Ag dopes or Ag–S codopes in ZnO, the intensity of the 2.06 eV band decreases greatly and no other band, for example, V_O band, is observed in the visible region, as shown in PL

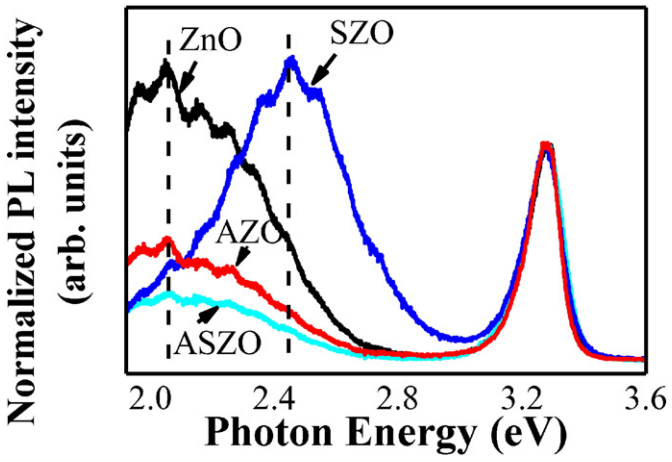

Fig. 5. Room temperature normalized photoluminescence spectra of the ZnO, AZO, SZO and ASZO films. The UV peaks are normalized.

spectra denoted by ASZ and ASZO, moreover, the intensity of the 2.06 eV band for the Ag–S codoped ZnO is smaller than that for the Ag-doped ZnO. In addition, accompanied by the decrease in the intensity of the 2.06 eV band, the Zn content also decreases, as shown in Table 3. These mean that the amount of Zn_i donor decreases greatly as Ag dopes into ZnO, at the same time, no other donor defects (such as V_O) form, that is, Ag doping can suppress the formation of both Zn_i and V_O donors, which will decrease compensation intrinsic donor for Ag_{Zn}^{+} and Ag_{Zn}^{+}–nS_O^{2-} acceptors. This result differs from that of AZO-MS and ASZO-MS, where Ag doping can suppress the formation of Zn_i but V_O, leading to that AZO-MS has high electron density (10^{17} cm^{-3}).

According to the above discussions, the formation of the p-type ASZO with high hole density and reproducibility can be attributed to follows: 1. formation of the Ag_{Zn}^{+}–nS_O^{2-} with an ionization energy smaller than that of Ag_{Zn}^{+}, the hole of p-type ASZO comes mainly from contribution of the Ag_{Zn}^{+}–nS_O^{2-} complex acceptor. 2. Increase in Ag doping concentration induced by S doping, which makes the ASZO have more Ag_{Zn}^{+} and Ag_{Zn}^{+}–nS_O^{2-} acceptors, and 3. suppress of the formation of Zn_i and V_O induced by Ag doping, which reduces compensation of intrinsic donors for Ag_{Zn}^{+} and Ag_{Zn}^{+}–nS_O^{2-} acceptors. Compared to ASZO-MS, the high hole density and reproducibility of the p-type ASZO are mainly due to the fact that Ag doping suppresses the formation of Zn_i and V_O donors.

4. Conclusions

The p-type ASZO films with a hole density of 10^{18} cm^{-3} were prepared reproducibly by the modified hydrothermal method, where the alkali solution is separated from reaction solution and O_2 is removed from the autoclave to avoid deoxidization of Ag^{+} and oxidization of S^{2-}. The Ag substitutes for the Zn site in the chemical state of Ag_{Zn}^{+} and the S occupies the O site in the state of S_O^{2-} in the ASZO. Some of the Ag_{Zn}^{2+} are surrounded by $4O^{2-}$ to form Ag_{Zn}^{+} acceptor and the other Ag_{Zn}^{1+} are surrounded by nS_O^{2-} to form Ag_{Zn}^{+}–nS_O^{2-} complex acceptor with an ionization energy smaller than that of Ag_{Zn}^{+}. Ag doping can suppress the formation of Zn_i and V_O donors in the ASZO, which leads to dramatic decreases in electron concentration from 10^{18} cm^{-3} of the ZnO to 10^{15} cm^{-3} and to reduce compensation of intrinsic donors for acceptors; S doping can increase Ag doping content in ZnO.

The formation of the p-type ASZO with high hole density and reproducibility is mainly attributed to a decrease in the amount of Zn_i and V_O induced by Ag doping and the formation of shallow Ag_{Zn}^{+}–nS_O^{2-} complex acceptor induced by the S doping. Compared to the p-type ASZO-MS, the improvement in the hole density of the p-type ASZO is due to a decrease in the amount of Zn_i and V_O induced by Ag doping.

Acknowledgments

This work is supported by the National Natural Science Foundation of China under Grant Nos. 10874178, 11074093, 61205038 and 11274135, Specialized Research Fund for the Doctoral Program of Higher Education under Grant No. 20130061130011, Ph.D. Programs Foundation of Ministry of Education of China under Grant No. 20120061120011, and National Found for Fostering Talents of Basic Science under grant No. J1103202.

References

[1] S. Yamamoto, Photoenhanced band-edge luminescence in ZnO nanocrystals dispersed in ethanol, J. Phys. Chem. C 115 (2011) 21635–21640.
[2] Y. Li, B. Yao, R. Deng, B. Li, Z. Zhang, C. Shan, D. Zhao, D. Shen, A comparative study on electroluminescence from ZnO-based double heterojunction light emitting diodes grown on different lattice mismatch substrates, J. Alloys Compd. 575 (2013) 233–238.
[3] Y.-Y. Lai, Y.-P. Lan, T.-C. Lu, Strong light–matter interaction in ZnO microcavities, Light Sci. Appl. 2 (2013), e76.
[4] Y.F. Li, B. Yao, Y.M. Lu, Z.P. Wei, Y.Q. Gai, C.J. Zheng, Z.Z. Zhang, B.H. Li, D.Z. Shen, X.W. Fan, et al., Realization of p-type conduction in undoped $Mg_xZn_{1-x}O$ thin films by controlling Mg content, Appl. Phys. Lett. 91 (2007) (232115).
[5] Y. Li, R. Deng, B. Yao, G. Xing, D. Wang, T. Wu, Tuning ferromagnetism in $Mg_xZn_{1-x}O$ thin films by band gap and defect engineering, Appl. Phys. Lett. 97 (2010) 102506.
[6] Q. Qiao, B.H. Li, C.X. Shan, J.S. Liu, J. Yu, X.H. Xie, Z.Z. Zhang, T.B. Ji, Y. Jia, D.Z. Shen, Light-emitting diodes fabricated from small-size ZnO quantum dots, Mater. Lett. 74 (2012) 104–106.
[7] Y. Li, R. Deng, W. Lin, Y. Tian, H. Peng, J. Yi, B. Yao, T. Wu, Electrostatic tuning of Kondo effect in a rare-earth-doped wide-band-gap oxide, Phys. Rev. B 87 (2013) 155151.
[8] A. Osinsky, J.W. Dong, M.Z. Kauser, B. Hertog, A.M. Dabiran, P.P. Chow, S.J. Pearton, O. Lopatiuk, L. Chernyak, MgZnO/AlGaN heterostructure light-emitting diodes, Appl. Phys. Lett. 85 (2004) 4272–4274.
[9] Y.F. Li, H.L. Pan, B. Yao, R. Deng, Y. Xu, J.C. Li, L.G. Zhang, H.F. Zhao, D.Z. Shen, T. Wu, Hole-mediated ferromagnetic enhancement and stability in Cu-doped ZnOs alloy thin films, J. Phys. D 45 (2012) (075002).
[10] Q.H. Zheng, D. Zhang, J. Huang, Y.H. Wang, F. Huang, Integrating surface textures on ZnO substrate for high light extraction efficiency light-emitting diode, J. Phys. Chem. C 118 (2014) 14894–14898.
[11] Y.F. Li, B. Yao, R. Deng, B.H. Li, J.Y. Zhang, Y.M. Zhao, D.Y. Jiang, Z.Z. Zhang, C.X. Shan, D.Z. Shen, et al., Ultraviolet photodiode based on p-Mg0.2Zn0.8O/n-ZnO heterojunction with wide response range, J. Phys. D 42 (2009) (105102).
[12] O. Lupan, B. Viana, T. Pauporte, M. Dhaouadi, F. Pelle, L. Devys, T. Gacoin, Controlled mixed violet–blue–red electroluminescence from Eu:nano-phosphors/ZnO-nanowires/p-GaN light-emitting diodes, J. Phys. Chem. C 117 (2013) 26768–26775.
[13] W.W. Liu, B. Yao, B.H. Li, Y.F. Li, J. Zheng, Z.Z. Zhang, C.X. Shan, J.Y. Zhang, D.Z. Shen, X.W. Fan, MgZnO/ZnO p–n junction UVphotodetector fabricated on sapphire substrate by plasma-assisted molecular beam epitaxy, Solid State Sci. 12 (2010) 1567–1569.
[14] Y.F. Li, B. Yao, Y.M. Lu, C.X. Cong, Z.Z. Zhang, Y.Q. Gai, C.J. Zheng, B.H. Li, Z.P. Wei, D.Z. Shen, et al., Characterization of biaxial stress and its effect on optical properties of ZnO thin films, Appl. Phys. Lett. 91 (2007) (021915).
[15] W. Liu, B. Yao, Y. Li, B. Li, C. Zheng, B. Zhang, C. Shan, Z. Zhang, J. Zhang, D. Shen, Annealing temperature dependent electrical and optical properties of ZnO and MgZnO films in hydrogen ambient, Appl. Surf. Sci. 255 (2009) 6745–6749.
[16] B. Zhang, B. Yao, S. Wang, Y. Li, C. Shan, J. Zhang, B. Li, Z. Zhang, D. Shen, Influence of Zn/O ratio on structural, electrical and optical properties of ZnO thin films fabricated by plasma-assisted molecular beam epitaxy, J. Alloys Compd. 503 (2010) 155–158.
[17] X. Fang, J. Li, D. Zhao, D. Shen, B. Li, X. Wang, Phosphorus-doped p-type ZnO nanorods and ZnO nanorod p—n homojunction LED fabricated by hydrothermal method, J. Phys. Chem. C 113 (2009) 21208–21212.
[18] C.H. Park, S.B. Zhang, S.-H. Wei, Origin of p-type doping difficulty in ZnO: the impurity perspective, Phys. Rev. B 66 (2002) (073202).
[19] N.Y. Garces, N.C. Giles, L.E. Halliburton, G. Cantwell, D.B. Eason, D.C. Reynolds, D.C. Look, Production of nitrogen acceptors in ZnO by thermal annealing, Appl. Phys. Lett. 80 (2002) 1334.
[20] Y.R. Ryu, T.S. Lee, H.W. White, Properties of arsenic-doped p-type ZnO grown by hybrid beam deposition, Appl. Phys. Lett. 83 (2003) 87.
[21] W. Li, C. Kong, H. Ruan, G. Qin, L. Fang, X. Meng, H. Zhang, P. Zhang, Q. Xu, Investigation on the formation mechanism of In–N codoped p-type ZnCdO thin films: experiment and theory, J. Phys. Chem. C 118 (2014) 22799–22806.
[22] X.H. Wang, B. Yao, D.Z. Shen, Z.Z. Zhang, B.H. Li, Z.P. Wei, Y.M. Lu, D.X. Zhao, J.Y. Zhang, X.W. Fan, et al., Optical properties of p-type ZnO doped by lithium and nitrogen, Solid State Commun. 141 (2007) 600–604.
[23] Y. Yan, M.M. Al-Jassim, S.-H. Wei, Doping of ZnO by group-IBelements, Appl. Phys. Lett. 89 (2006) 181912.
[24] C. Persson, C. Platzer-Björkman, J. Malmström, T. Törndahl, M. Edoff, Strong valence-band offset bowing of $ZnO_{1-x}S_x$ enhances p-type nitrogen doping of ZnO-like alloys, Phys. Rev. Lett. 97 (2006) 146403.
[25] L.J. Sun, J. Hu, H.Y. He, X.P. Wu, X.Q. Xu, B.X. Lin, Z.X. Fu, B.C. Pan, Effects of S incorporation on Ag substitutional acceptors in ZnO:(Ag, S) thin films, Solid State Commun. 149 (2009) 1663–1665.
[26] J.C. Li, Y.F. Li, T. Yang, B. Yao, Z.H. Ding, Y. Xu, Z.Z. Zhang, L.G. Zhang, H.F. Zhao, D.Z. Shen, Effects of S on solid solubility of Ag and electrical properties of Ag-doped ZnO films grown by radio frequency magnetron sputtering, J. Alloys Compd. 550 (2013) 479–482.
[27] Y.F. Wang, J.H. Yao, G. Jia, H. Lei, Optical prosperities of Ag–ZnO composition nanofilm synthesized by chemical bath deposition, Acta Phys. Pol. A 119 (2011) 451–454.
[28] M. Patra, A. Padhye, M. Manoth, G. Gowd, V. Singh, S.R. Vadera, N. Kumar, Growth and studies of S2-doped ZnO nanorods by solution growth technique, Adv. Mater. Res. 67 (2009) 239–244.
[29] R. Chen, C. Zou, J. Bian, A. Sandhu, W. Gao, Microstructure and optical properties of Ag-doped ZnO nanostructures prepared by a wet oxidation doping process, Nanotechnology 22 (2011) 105706.
[30] Y. Jin, Q. Cui, K. Wang, J. Hao, Q. Wang, J. Zhang, Investigation of photoluminescence in undoped and Ag-doped ZnO flowerlike nanocrystals, J. Appl. Phys. 109 (2011) 053521.
[31] Y. Xu, T. Yang, B. Yao, Y.F. Li, Z.H. Ding, J.C. Li, H.Z. Wang, Z.Z. Zhang, L.G. Zhang, H.F. Zhao, et al., Influence of Ag–S codoping on silver chemical states and stable p-type conduction behavior of the ZnO films, Ceram. Int. 40 (2014) 2161–2167.
[32] C.H. Ahn, Y.Y. Kim, D.C. Kim, S.K. Mohanta, H.K. Cho, A comparative analysis of deep level emission in ZnO layer deposited by various methods, J. Appl. Phys. 105 (2009) (089902).
[33] M.S. Kim, G. Nam, S. Kim, D.Y. Kim, D.-Y. Lee, J.S. Kim, S.-O. Kim, J.S. Kim, J.-S. Son, J.-Y. Leem, Photoluminescence studies of ZnO thin films on R-plane sapphire substrates grown by sol–gel method, J. Lumin. 132 (2012) 2581–2585.